Int. J. Solids Structures Vol. 29, No. 17, pp. 2181–2200, 1992
Printed in Great Britain.

0020–7683/92 $5.00 + .00
Pergamon Press Ltd

HOMOGENIZED NONLINEAR CONSTITUTIVE PROPERTIES AND LOCAL STRESS CONCENTRATIONS FOR COMPOSITES WITH PERIODIC INTERNAL STRUCTURE

STEFAN JANSSON
Department of Mechanical and Environmental Engineering, University of California, Santa Barbara, CA 93106, U.S.A.

(*Received* 2 *March* 1991; *in revised form* 14 *December* 1991)

Abstract—A unit cell problem governing effective mechanical properties and local stress concentrations for composites with periodic micro-structure and nonlinear constituents has been derived by employing an asymptotic expansion of the field variables in two length-scales. The influence of cell type upon effective properties has been investigated for a continuous fiber reinforced composite. It was found that the effective transverse properties are strongly dependent on the unit cell type when the matrix exhibits a nonlinear response. Finally the anisotropic behavior of the hexagonal unit cell and its applicability to determine effective properties and initial yield surface for transversely isotropic composites has been investigated.

1. INTRODUCTION

A common problem in the mechanics of composites is to determine effective properties for a composite from the distribution and properties of the constituents. This may be necessary because sufficient data are not available for a system. Traditionally, only the inplane properties have been reported for laminates. Many new composites are only available in limited quantities and this restricts the properties that can be determined experimentally. However, the recent consideration of composites in new demanding applications with new design problems requires more information in order to determine stress concentrations, interlaminar stresses and edge effects. Furthermore, the properties of a hypothetical composite which has not been manufactured could be required in order to make early design decisions or to tailor a composite for specific application. Sometimes all the properties of the constituents are known and the effective properties can be calculated directly. Quite often some of the properties of the constituents are unknown, or the properties of the constituents in the composite differ from their bulk properties, and have to be determined from the properties of the composite by back-calculations.

Effective properties for linear elastic composites have been addressed extensively and access to the literature is provided in Jones (1974), Christensen (1979) and Hashin (1983). One group of the methods uses the solution for the stress and strain fields for a single reinforcement embedded in an infinite body and the influence of the different reinforcements are accounted for by superposition. Average stresses and strains can be readily calculated and the effective material constants can be determined. In the dilute scheme, the reinforcements are assumed to be in an infinite body with the properties of the matrix and so far apart that they do not interact. Closed form solutions can usually be obtained but their validity is restricted to low volume fractions of reinforcements. This restriction is eased somewhat in the self-consistent scheme where the reinforcements are assumed to be embedded in an infinite body with the properties of the composite. Iterative numerical procedures are often required to calculate the effective properties. The results are valid for higher volume fractions than the results for the dilute scheme. In the differential schemes the dilute solution for a small perturbation of reinforcements in an infinite body is used. It is expected that this solution is very accurate. The governing equations for the effective properties are then integrated from zero volume fraction of reinforcement up to the actual volume fraction by letting the properties of the surrounding body change gradually from matrix to composite. Numerical integration is often needed. The results are close to self-consistent

results but usually predict a somewhat more compliant composite. Energy methods can also be employed to form upper and lower bounds for the effective properties. The bounds are usually too far apart to be really useful for predicting effective properties with the accuracy that is needed for structural calculations. Simple geometrical models, like the cylinder model for continuous fiber reinforced composites, have the advantage of permitting closed form solutions and sometimes give excellent results.

The methods mentioned above do not account for the local interaction between neighboring reinforcements and could not be expected to give accurate results for high volume fractions of reinforcement. This case is usually analysed by assuming that the composite material has a periodic microstructure and a small unit cell can be identified. The analysis often requires numerical methods. In a real material the reinforcements are usually randomly distributed in some planes and the concern is how well the artificially periodic material resembles the real material. Experience of the linear elastic properties of fiber reinforced systems (Adams and Tsai, 1969), indicates that the choice of unit cell is not critical and does not affect the effective properties noticeably. The same experience is not available for composites with nonlinear constituents even if some limited results exist (Adams, 1970).

The method of homogenization is used here to derive a solution to the problem of the unit cell that govern effective properties and local stress and strain concentrations for composites with nonlinear constituents. The method is a two-space method that was used by Larson (1976) to study neutron transportation in inhomogeneous media and has been discussed by Keller (1976). Len'e and Leguillon (1982) and Len'e (1986) used it to calculate effective properties for composites with linear elastic constituents. The complexity of representing the state of the composite with a limited number of global state variables has been addressed in conjunction with the method by Suquet (1983, 1985). First the theory of homogenization is used to show that the leading order problem for the effective properties is a standard boundary value problem defined on the unit cell with periodical boundary conditions. The solution procedure required for the effective properties has been implemented in a finite element program. Finally, it is studied how the unit cell type and loading directions affect effective properties and stress concentrations for a unidirectional continuous fiber-reinforced metal matrix composite.

2. HOMOGENIZATION

2.1. *Statement of the problem*

Consider a periodic nonlinear elastic inhomogeneous body, Fig. 1, which comprises at least two constituents. The body has two length scales, a global length scale, D, that is of

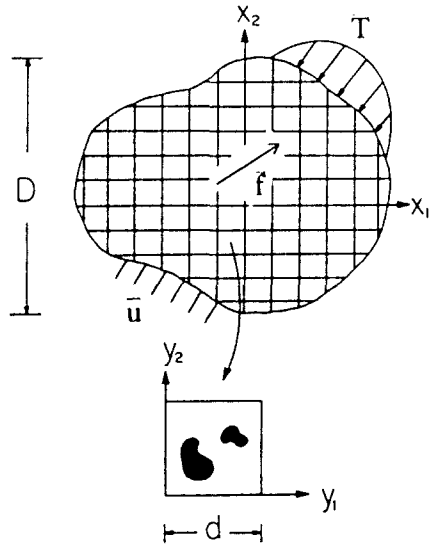

Fig. 1. Periodic body and representative unit cell.

the order of the size of the body, and a local length scale, d, that is proportional to the wavelength of the variation of the micro-structure. The micro-structure is periodic and it is sufficient to specify the distribution of the constituents on the smallest repeatable element, the unit cell. The size of the unit cells is further assumed to be much smaller than the size of the body so that,

$$\delta = \frac{d}{D} \ll 1. \tag{1}$$

The relation between the global coordinate system x_i for the body and the local y_i for the unit cell can then be written as

$$y_i = \frac{x_i}{\delta} \tag{2}$$

where δ is the scaling between the two length scales. A movement of order unity on the local scale corresponds to a very small movement on the global scale.

The coefficients $C_{ijkl}(\varepsilon, y)$ in the nonlinear constitutive equations (3b) are assumed to have the usual symmetry properties and are functions of the position y_i and the invariant of the strain tensor ε_{ij}. The spatial dependence of the coefficients in the unit cell is given through the distribution of the constituents. Furthermore, the wavelengths of the prescribed traction $\bar{T}_i$, displacements $\bar{u}_i$ and body forces $\bar{f}_i$ will be restricted to being much longer than the wavelength of the micro-structure in order to allow for a homogenized solution, e.g. no point loads are allowed. This defines the boundary value problem (3) for the composite structure from which the unknown field quantities, stress σ_{ij}, strain ε_{ij} and displacements u_i can be solved for:

$$\sigma_{ij,j} + \bar{f}_i = 0 \quad \text{in} \quad V, \qquad \sigma_{ij} = C_{ijkl}\left(\frac{x}{\delta}, \varepsilon\right)\varepsilon_{kl}, \qquad \varepsilon_{kl} = \tfrac{1}{2}(u_{k,l} + u_{l,k}) \tag{3a-c}$$

$$\sigma_{ij} n_j = \bar{T}_i \quad \text{on} \quad S_\sigma, \qquad u_i = \bar{u}_i \quad \text{on} \quad S_u. \tag{3d,e}$$

This boundary value problem has the feature that $C_{ijkl}(\varepsilon, x/\delta)$ varies very rapidly with a short wavelength on the global length scale x_i and it is hard to find a solution that solves the global problem and accounts for the local oscillation at the same time. Hence, there is a motivation to look for a simplified solution.

2.2. *Asymptotic expansion*

Assume a solution of the field variables could be found that is a function of the two space variables x_i and y_i and depends regularly upon δ. Hence, it is natural to look for an asymptotic expansion of the displacement field in the form

$$u_i(x, y, \delta) = u_i^0(x, y) + \delta u_i^1(x, y) + \delta^2 u_i^2(x, y) + \cdots \tag{4a}$$

where $u_i^n(x, y)$ is a slowly varying function in x_i due to the restriction of the loading and a periodic function in y_i governed by the periodicity of the micro-structure,

$$u_i^n(x, y) = u_i^n(x, y + d). \tag{4b}$$

The boundary conditions can be expanded in a similar way

$$\bar{u}_i(x, y, \delta) = \bar{u}_i^0(x, y) + \delta \bar{u}_i^1(x, y) + \delta^2 \bar{u}_i^2(x, y) + \cdots \tag{5a}$$

$$\bar{T}_i(x, y, \delta) = \bar{T}_i^0(x, y) + \delta \bar{T}_i^1(x, y) + \delta^2 \bar{T}_i^2(x, y) + \cdots \tag{5b}$$

$$\bar{f}_i(x, y, \delta) = \bar{f}_i^0(x, y) + \delta \bar{f}_i^1(x, y) + \delta^2 \bar{f}_i^2(x, y) + \cdots \tag{5c}$$

Use of the definition for strain (3c) together with differentiation with respect to the two length scales on (4a) gives

$$\varepsilon_{ij} = \tfrac{1}{2}(u_{i,x_j} + u_{j,x_i}) + \frac{1}{2\delta}(u_{i,y_j} + u_{j,y_i}) = \tfrac{1}{2}\Big[(u^0_{i,x_j} + u^0_{j,x_i}) + \delta(u^1_{i,x_j} + u^1_{j,x_i}) + \delta^2(u^2_{i,x_j} + u^2_{j,x_i}) + \cdots + \frac{1}{\delta}(u^0_{i,y_j} + u^0_{j,y_i}) + (u^1_{i,y_j} + u^1_{j,y_i}) + \delta(u^2_{i,y_j} + u^2_{j,y_i}) + \cdots\Big]. \quad (6)$$

The stress can now be derived from the constitutive equation (3b) by using the expression for the strain (6) as

$$\sigma_{ij} = \sigma^0_{ij} + \sigma^1_{ij} + \sigma^2_{ij} + \cdots \quad (7a)$$

where the different orders of the stress are

$$\sigma^0_{ij} = C_{ijkl}(y, \varepsilon)\frac{1}{2\delta}(u^0_{k,y_l} + u^0_{l,y_k}), \qquad \sigma^1_{ij} = C_{ijkl}(y, \varepsilon)\tfrac{1}{2}(u^0_{k,x_l} + u^0_{l,x_k} + u^1_{k,y_l} + u^1_{l,y_k}) \quad (7b,c)$$

$$\sigma^2_{ij} = C_{ijkl}(y, \varepsilon)\delta\tfrac{1}{2}(u^1_{k,x_l} + u^1_{l,x_k} + u^2_{k,y_l} + u^2_{l,y_k}) \quad (7d)$$

$$+ \frac{\partial C_{ijkl}(y, \varepsilon)}{\partial \varepsilon_{rs}}\frac{\partial}{4}(u^0_{k,x_l} + u^0_{l,x_k} + u^1_{k,y_l} + u^1_{l,y_k})(u^1_{r,x_s} + u^1_{s,x_r} + u^2_{r,y_s} + u^2_{s,y_r}). \quad (7e)$$

Differentiation of the equilibrium equation (3a) with respect to the two length scales gives

$$\sigma_{ij,x_j} + \frac{1}{\delta}\sigma_{ij,y_j} + f_i = 0. \quad (8)$$

Inserting the expression for the stress (7) in the equilibrium equation (8) and identifying the terms of different order in δ gives

$$\sigma^0_{ij} = 0 \quad O\left(\frac{1}{\delta^2}\right), \qquad \sigma^1_{ij,y_j} + \sigma^0_{ij,x_j} = 0 \quad O\left(\frac{1}{\delta}\right), \qquad \sigma^2_{ij,y_j} + \sigma^1_{ij,x_j} + f_i = 0 \quad O(1) \quad (9a\text{-}c)$$

and equations of higher order in δ. There are no boundary conditions associated with eqn (9a). It can be satisfied by letting the leading order term of the displacement

$$u^0_i = u^0_i(x).$$

It is also required in order to avoid singularities in the strain, eqn (6). In (7b) this implies that

$$\sigma^0_{ij} \equiv 0$$

and eqn (9b) simplifies to

$$\sigma^1_{ij,y_j} = [C_{ijkl}(\varepsilon^0 + \varepsilon^1)]_{,y_j} = 0 \quad (10)$$

where the first term of the strain

$$\varepsilon^0_{ij}(x) = \tfrac{1}{2}[u^0_{i,x_j}(x) + u^0_{j,x_i}(x)] \quad (11)$$

is constant over the unit cell and the second term

$$\varepsilon_{ij}^1(x, y) = \tfrac{1}{2}[u_{i,y_j}^1(x, y) + u_{j,y_i}^1(x, y)] \tag{12}$$

is a periodic function on the unit cell.

The equilibrium equation (10) together with the definitions of strain (11) and (12) and the periodicity requirement of the displacement field (4b) form a well-posed boundary value problem on the unit cell for the displacement field u_i^1 when the displacement field is fixed at some location in the unit cell and ε_{ij}^0 is given. The solution to the problem can be written formally as

$$u_i^1 = B_{ikl}(y, \varepsilon^0)\varepsilon_{kl}^0, \qquad \varepsilon_{ij}^1 = A_{ijkl}(y, \varepsilon^0)\varepsilon_{kl}^0 \tag{13, 14}$$

$$\sigma_{ij}^1 = [C_{ijkl} + C_{ijpq}A_{pqkl}]\varepsilon_{kl}^0 \tag{15}$$

and the average strain in the unit cell can be calculated as

$$\langle \varepsilon_{ij} \rangle = \frac{1}{Y}\int_Y (\varepsilon_{ij}^0 + \varepsilon_{ij}^1)\, \mathrm{d}Y = \varepsilon_{ij}^0 + \frac{1}{Y}\int_\Gamma \tfrac{1}{2}(u_i^1 n_j + u_j^1 n_i)\, \mathrm{d}\Gamma = \varepsilon_{ij}^0. \tag{16}$$

The first term ε_{ij}^0 is constant. The divergence theorem together with the definition of strain have been used on the second term ε_{ij}^1. The resulting surface integral is zero because the displacement field u_i^1 is periodic and equal on the opposite sides of the unit cell while the normal n_j has opposite directions. The average stress in the unit cell could formally be calculated and expressed as a function of the average strain as

$$\langle \sigma_{ij}^1 \rangle = [\langle C_{ijkl} \rangle + \langle C_{ijpq}A_{pqkl} \rangle]\varepsilon_{kl}^0 = Q_{ijkl}(\varepsilon^0)\varepsilon_{kl}^0. \tag{17}$$

Taking the average over the unit cell of the equilibrium equation of order unity (9c) yields

$$\langle \sigma_{ij,y_i}^2 \rangle + \langle \sigma_{ij,x_i}^1 \rangle + \langle f_i \rangle = 0.$$

Use of the divergence theorem on the first term gives

$$\langle \sigma_{ij,y_i}^2 \rangle = \frac{1}{Y}\int_\Gamma \sigma_{ij}^2 n_j\, \mathrm{d}\Gamma = 0 \tag{18}$$

because the periodicity of the displacement field causes σ_{ij}^2 to be periodic and contributions form opposite sides on the boundary of the unit cell canceling each other out. The leading order terms of the series expansions of the boundary conditions (5a,b) and the volume force (5c) can only be functions of the global length scale due to the restriction made on the displacement field (4a). The leading order terms are then equal to the average of the field variables over the unit cell. The global boundary value problem for averages of the field variables on the unit cell then reads

$$\langle \sigma_{ij}^1 \rangle_{,x_j} + f_i^0(x) = 0 \quad \text{in} \quad V, \qquad \varepsilon_{ij}^0 = \tfrac{1}{2}(u_{i,x_j}^0 + u_{j,x_i}^0), \tag{18a,b}$$

$$u_i^0 = \bar{u}_i^0(x) \quad \text{on} \quad S_u, \qquad \langle \sigma_{ij}^1 \rangle n_j = \bar{T}_i^0(x) \quad \text{on} \quad S_\sigma \tag{18c,d}$$

where the effective constitutive equation (17) is given by the solution of the problem defined on the unit cell. It can be seen from the asymptotic expansion (4a) that the solution of the displacement field goes to the correct one when $\delta \to 0$, the size of the unit cell goes to zero in relation to the size of the body. However the errors in local variation of stress and strain on the unit cell depend on the stress concentrations and are in general not bounded while the average values tend to the correct solution. The accuracy of the solution can be improved

by including higher order terms when the variation in the boundary conditions is strong over a unit cell length. However, this is hardly a practical procedure for the nonlinear case.

2.3. *Numerical implementation*

The remaining part of the report focuses on calculations of effective properties and local stress concentrations. The unknown displacement u_i^1, which is periodic on the unit cell (4b), is determined by solving the equilibrium equation (10) for a given strain ε_{ij}^0, which is constant over the unit cell. The local stress concentration is given by (15) and the average stress is calculated by integrating (15) over the unit cell and the effective stress strain relation for the composite is given by (17).

The numerical solution of the unit cell problem requires a variational formulation of the equilibrium equation (10). Multiplying (10) with the variation of the displacement field $\mathrm{d}u_i^1$, integration over the unit cell and use of the divergence theorem gives

$$\int_Y \sigma_{ij,j}^1 \delta u_i^1 \,\mathrm{d}Y = \int_\Gamma \sigma_{ij}^1 n_j \delta u_i^1 \,\mathrm{d}\Gamma - \int_Y \sigma_{ij} \delta u_{i,j}^1 \,\mathrm{d}Y = 0 \tag{19}$$

where the term

$$\int_\Gamma \sigma_{ij}^1 \delta u_i^1 n_j \,\mathrm{d}\Gamma = 0.$$

Hence, the last of eqn (19) together with definition of stress (7c) and strain (11) and (12) give the final form

$$\int_Y C_{ijkl}(\varepsilon)\varepsilon_{ij}^1 \delta\varepsilon_{ij}^1 \,\mathrm{d}Y = -\int_Y C_{ijkl}(\varepsilon)\varepsilon_{ij}^0 \delta\varepsilon_{ij}^1 \,\mathrm{d}Y. \tag{20}$$

This formulation has been implemented in a finite element program for a two dimensional distribution of reinforcements.

The constituent's behavior has been described by a J_2 deformation theory, *cf.* Hutchinson and Neal (1981). The total strain ε_{ij}^1 is given as the sum of the elastic component

$$\varepsilon_{ij}^e = \frac{1+\nu}{E}\sigma_{ij} - \frac{\nu}{E}\sigma_{kk}\delta_{ij} \tag{21a}$$

and a nonlinear plastic component

$$\varepsilon_{ij}^p = \frac{3}{2}\left(\frac{1}{E_s} - \frac{1}{E}\right)s_{ij} \tag{21b}$$

where E is Young's modulus, ν the Poisson's ratio and s_{ij} the stress deviator. The secant modulus is given as $E_s = \sigma_e/\varepsilon_e$ where σ_e is the von Mises equivalent stress and ε_e is the associated equivalent strain. The stress–strain relation reduces to

$$\varepsilon = \begin{cases} \dfrac{\sigma}{E} & \sigma < \sigma_o \\ \dfrac{\sigma_o}{E}\left(\dfrac{\sigma}{\sigma_o}\right)^n & \sigma \geqslant \sigma_o \end{cases} \tag{22}$$

in uniaxial tension, where σ_o is the yield stress.

The displacement field is interpolated with nine node isoparametric elements. Selective reduced integration is used to avoid locking, 2×2 is used for the hydrostatic component and 3×3 is used for the deviatoric component of the stress field. The nonlinear system of equations is solved with a Newton–Raphson scheme extended with line search (Jansson, 1986). The program can handle periodic boundary conditions as well as different symmetry conditions. An outer Newton–Raphson loop solves for ε_{33}^0 when a condition on the average stress in the 3-direction is imposed. The averages of stresses and strains are calculated by numerical integration at the Gauss points.

The described implementation requires access to the source code of a finite element program. This is not always available. The given strain ε_{ij}^0 in (20) can be converted to an equivalent condition for the displacements on the boundary by using the complementary virtual work theorem. The requirement of periodicity of the displacement field on the boundary is replaced with

$$u_i(x, y+d) = \varepsilon_{ij}^0 d_j + u_i(x, y). \tag{23}$$

The average stress can also be evaluated from the nodal reactions by use of the divergence theorem as

$$\int_Y y_k \sigma_{ij,j}\, \mathrm{d}Y = \int_\Gamma y_k \sigma_{ij} n_j\, \mathrm{d}\Gamma - \int_Y y_{k,j} \sigma_{ij}\, \mathrm{d}Y = \int_\Gamma y_k \sigma_{ij} n_j\, \mathrm{d}\Gamma - \int_Y \sigma_{ik}\, \mathrm{d}Y.$$

For the unit cell problem $\sigma_{ij,j} = 0$ and

$$\int_Y \sigma_{ij}\, \mathrm{d}Y = \int_\Gamma y_i \sigma_{ik} n_k\, \mathrm{d}\Gamma \tag{24}$$

that is the mean stress theorem for the case of no body forces.

3. CASE STUDY

3.1. *Modeling*

The modeling of a high volume fraction fiber reinforced metal matrix composite is achieved by using the described procedure. The composite consists of a ductile aluminum alloy matrix reinforced with long stiff alumina fibers in an unidirectional lay-up. The bond between fiber and matrix is very strong. The basic properties of the composite and consistuents are given in Table 1. Detailed information and experimental procedures are reported in Jansson (1990). The fibers are nearly parallel in the longitudinal direction and randomly distributed in the transverse plane. This is very close to the assumption that the composite consists of fibers that are long parallel cylinders randomly distributed in the

Table 1. Comparison between experimentally measured elastic constants, calculated for different array types, and predictions by a commonly used method

	E_{11} GPa	E_{33} GPa	G_{12} GPa	G_{13} GPa	ν_{12}	ν_{31}	ν_{13}
Experiment	150	225	55	58	0.31	0.28	0.18
Homogenization:							
square array	159	220	49.3	57.9	0.283	0.284	0.205
hexagonal array	148	220	54.9	57.3	0.336	0.281	0.189
Engineering rules	160†	220‡	55§	57†	0.47§	0.29‡	0.21†‡
$E_f = 344.5$ GPa	$\nu_f = 0.26$						
$E_m = 68.9$ GPa	$\nu_m = 0.32$						
$c_m = 55\%$							

†Halpin–Tsai.
‡Rule of mixture.
§Cylinder model.

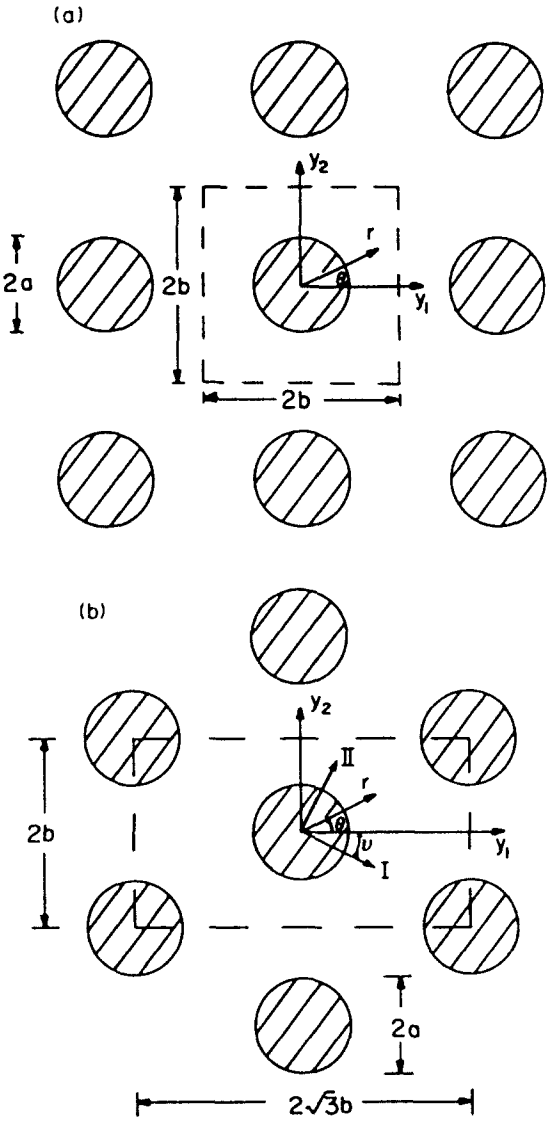

Fig. 2. Arrays with the representative unit cell indicated: (a) Square array. (b) Hexagonal array.

transverse plane. The problem is then reduced from three to two dimensions. The repeating element in the transverse plane is of a similar size to the composite, including many fibers, and is too complex for repeated numerical analysis, especially when the constituents have a nonlinear stress strain relation. Hence, the random distribution of fibers has to be approximated with a periodic distribution in order to reduce the size of the problem. It is not clear how well different periodic distributions model random distributions. Two different array types, a square Fig. 2a and a hexagonal array Fig. 2b, have been investigated. The choices of unit cells are also shown. It is not unique but the most convenient for the present calculations.

The loadings considered coincide with the principal directions of the material and only a quarter of the unit cell for the square array needs to be analysed because of symmetries. The hexagonal unit cell has an additional inversion symmetry around the point ($y_1 = \sqrt{3}/2\, b, y_2 = 1/2\, b$) that makes it possible to reduce the problem to an eighth of its original size. The boundary conditions are derived in Appendix A.

3.2. *Linear elastic behavior*

The calculated effective properties for the two array types are given in Table 1 together with experimental data for the composite in question. The results are also compared with

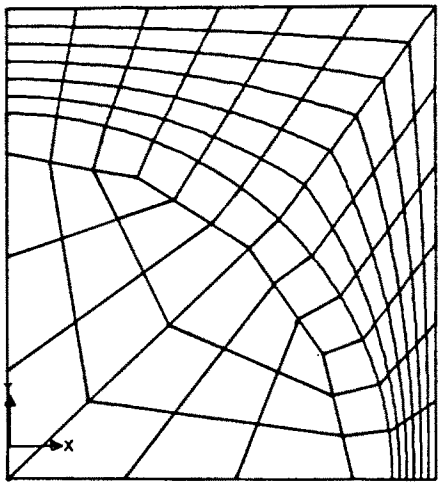

Fig. 3. Finite element mesh used for the analysis of the hexagonal array.

results of rules that are frequently used in engineering to estimate effective properties, *cf.* Jones (1974) and Christensen (1979). The longitudinal modulus E_{33} and the inplane Poisson's ratio ν_{13} are insensitive to the array types and are also given accurately by the rule of mixtures. The reason for this is that the mismatch in Poisson's ratio between fiber and matrix causes perturbation in the strain field that is of second order compared to the nominal strains and does not change the stored energy substantially. The inplane shear modulus G_{13} is also insensitive to the array types and is given closely by the Halpin–Tsai equation. The transverse modulus E_{11}, the transverse shear modulus G_{12}, and the Poisson's ratio ν_{12} are more sensitive to array type. The hexagonal array gives the best overall prediction of the transverse properties. The Halpin–Tsai equation gives a transverse modulus close to the prediction of the square array because it is semi-empirical and has been fitted to the results of a square array. The prediction of ν_{12} from the engineering rules shows that serious errors can occur if methods, based on different assumptions, are combined to calculate an elastic constant. It can be concluded that the use of the hexagonal unit cell provides a consistent method to calculate all the effective properties. Only five eight node isoparametric elements are needed in order to calculate the elastic constants with 1% accuracy. Hence, the computer-power needed is minimal and this scheme has been implemented successfully on a personal computer (Burns, 1989). The problem governing the linear elastic properties can also be solved efficiently by use of Fourier series (Chen and Cheng, 1967). The experiments and calculations indicate that the transverse shear modulus G_{12} is approximately equal to the inplane shear modulus G_{13}. This and the fact that the elements $C_{1122} = C_{1133}$ in the stiffness tensor were assumed by Christensen (1987) in order to simplify the transformations of the stiffness tensor. The number of independent constants are then reduced from five to three. Calculations show that the two assumptions are accurate within 10% for a wide range of volume fractions and modulus combinations when the fibers are isotropic.

3.3. *Nonlinear behavior*

The deformation characteristics have been studied for a hardening exponent $n = 5$ in the constitutive equation (23), which is a realistic value for a ductile metal matrix. A typical mesh is shown in Fig. 3. The nonlinear longitudinal properties were found to be insensitive to array type while the transverse properties and inplane shear responses were found to be sensitive to array type. Transverse stress strain curves for the different array types are shown in Fig. 4. As noted earlier, the linear elastic response is not greatly affected by the array type. The nonlinear response is substantially affected and the limit load for the square array is approximately twice as high as that of the hexagonal array for the present loading directions. It can also be seen from the graph that an assumption of plane strain in the fiber direction instead of generalized plane strain only affects the initial linear elastic response.

The transverse stress–strain curve could be estimated from the plane strain curve by adjusting the linear elastic strain component.

Since the predictions of the square and hexagonal arrays differ substantially, it is then a concern if any of the array types have the features which resemble the behavior of a real composite with randomly distributed fibers. Some insight into this is provided by the form of the invariants of the stress tensor for the different systems. The stress invariants reflect the symmetries of the mechanical properties. They are given in Appendix B for the two array types together with those for a transversely isotropic material that has the symmetry properties of a composite with randomly distributed fibers. The invariants of the hexagonal array and the transversely isotropic material agree up to second order. This implies that the linear elastic constants have the same symmetry properties because the energy function is quadratic in the stress components. The invariants of the square array agree only to first order with the invariants for the transversely isotropic material. This indicates that the square array could not be expected to resemble the behavior of a transversely isotropic material even for the linear elastic response.

The hexagonal array will be studied further because it has the symmetry properties closest to a transversely isotropic material. It will be found that the difference in high order terms of the hexagonal array and the transversely isotropic material is reflected by a directional dependence of the nonlinear response for transverse loadings and inplane shear.

The calculated longitudinal stress–strain curve for the hexagonal array is shown in Fig. 5. The deformation of the composite is dominated by the stiff fibers and the nonlinear contribution from the matrix enters as a small perturbation and the composite response appears to be bilinear. The plastic deformation of the matrix introduces a larger mismatch in Poisson's ratio between fiber and matrix than for the linear elastic response. The interaction in the transverse plane is still small and an identical stress–strain curve could be calculated by assuming a parallel system of fiber and matrix. The initial yield stress is also given closely by the parallel system.

The transverse stress–strain curves are shown in Fig. 6 for different loading directions. The initial yield stress and the nonlinear portion of the curves, especially the transition from linear to fully plastic behavior, are weakly dependent on the loading direction and the composite has a somewhat higher limit stress for σ_{11} loading. The transverse load carrying capacity is governed by the matrix flow stress strengthened by the plane strain condition in the 3-direction, induced by the continuous fibers, and by the constraint that the fibers induce on the inplane deformation.

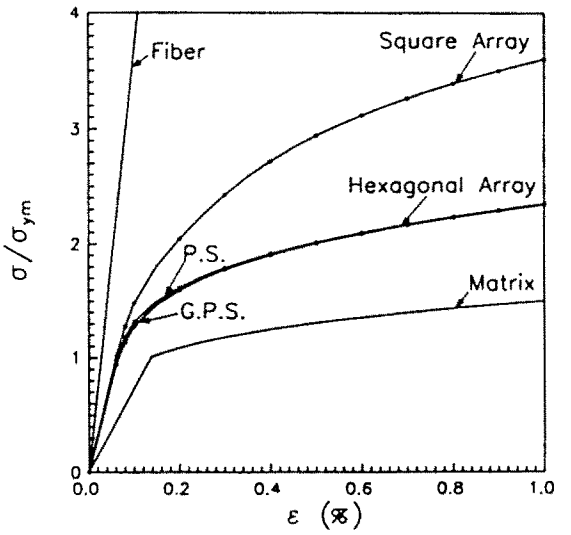

Fig. 4. Transverse stress–strain curves for loading in the x_1 direction. The square array has been analysed for generalized plane strain and the hexagonal array has been analysed for generalized plane strain.

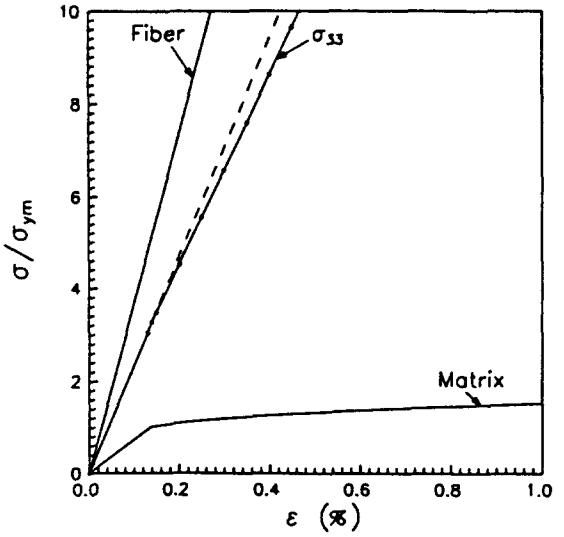

Fig. 5. Longitudinal stress–strain curve. Dashed line indicates initial elastic response.

The calculated shear stress strain curves are shown in Fig. 7. The loading τ_{12} is the only transverse shear stress that induces a pure shear strain response in the transverse plane because the principal stresses are oriented in directions with identical micro-structure. Loading in all other directions induces a combination of shear and normal strain and does not decouple transverse tension and shear in the way expected for a transversely isotropic material. The nonlinear inplane shear response, τ_{13} and τ_{23}, is dependent on the loading direction and the difference is more pronounced than for transverse tension, Fig. 6, and the limit stress for τ_{13} loading is noticeably lower than for τ_{23} loading. It can be seen in Fig. 2b that τ_{13} load planes parallel to the loading plane permit slip unconstrained by the fibers. This implies that the limit stress for a perfectly-plastic matrix is the same as the matrix yield stress in shear. In a large volume element of a composite with randomly distributed fibers, planes cut through fibers and the area fraction of fibers on the planes are equal to the volume fraction. The deformation for τ_{23} is constrained because no unconstrained planes exist in the 1–3 directions for the present volume fraction. Lower volume fractions will permit unconstrained slip for both loadings. Hence, the τ_{23} curve must be closer to the response of a composite with randomly distributed fibers than the τ_{13} curve. It should also be noted, Fig. 7, that the transverse shear stress–strain curve τ_{12} is remarkably similar to

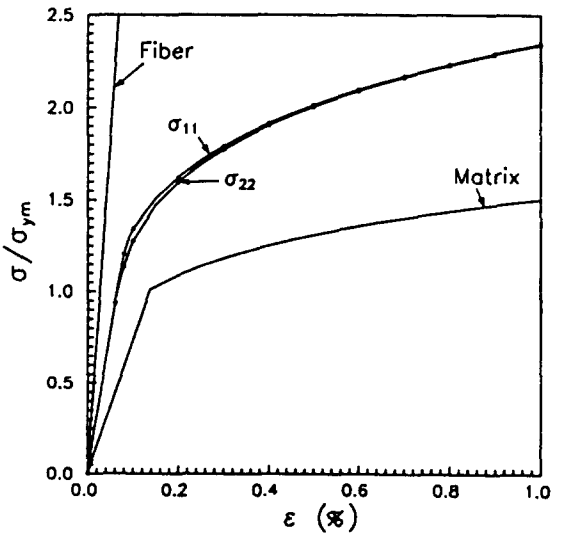

Fig. 6. Transverse stress–strain curves for loading in the y_1 and y_2 directions of the hexagonal array.

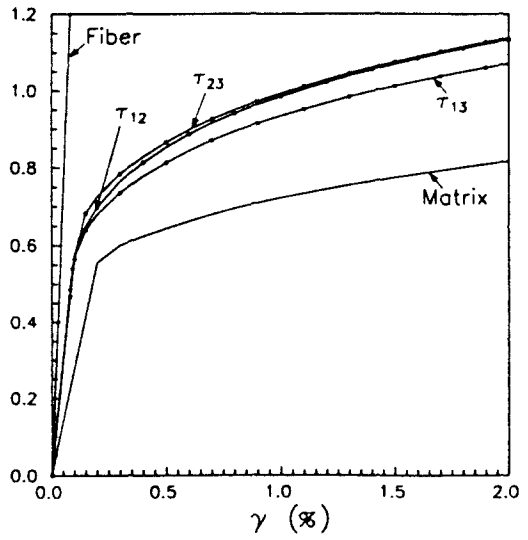

Fig. 7. Shear stress–strain curves for transverse shear σ_{12} and inplane shear σ_{13} and σ_{23}.

the inplane shear stress–strain curve τ_{13} and the responses can be assumed to be identical. This will provide a simplification of the macroscopic constitutive equations describing the composite behavior. However, this assumption remains to be verified experimentally.

3.4. *Hydrostatic tension*

The plastic deformation of metals is commonly accepted to be incompressible and this is used in the formulation of constitutive equations for continuous fiber reinforced metal matrix composites. The calculated response for hydrostatic loading, Fig. 8, shows that the plastic deformation occurs with an increase in volume. Furthermore, it is also quite unlikely that the average deformation of a body consisting of an elasto-plastic phase and a linear elastic phase would be incompressible. The nonlinearity for the hydrostatic loading is of the same magnitude as for longitudinal tension, Fig. 5. This indicates that if incompressibility is assumed in the formulation of the constitutive equations then inextensibility of the plastic deformation in the fiber direction must also be assumed in order to be consistent.

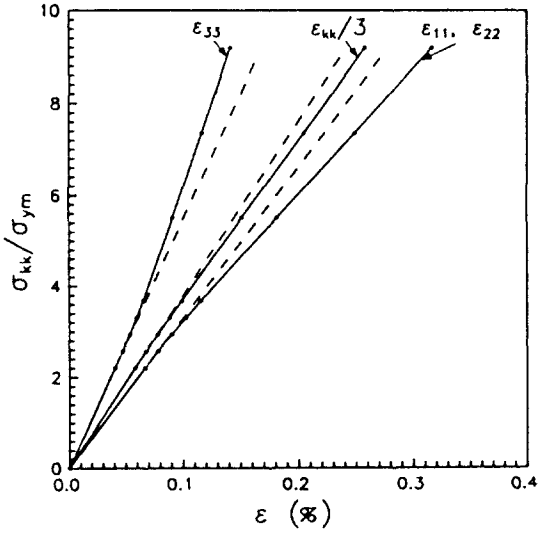

Fig. 8. Stress–strain curves for hydrostatic loading. Dashed lines indicate initial elastic responses.

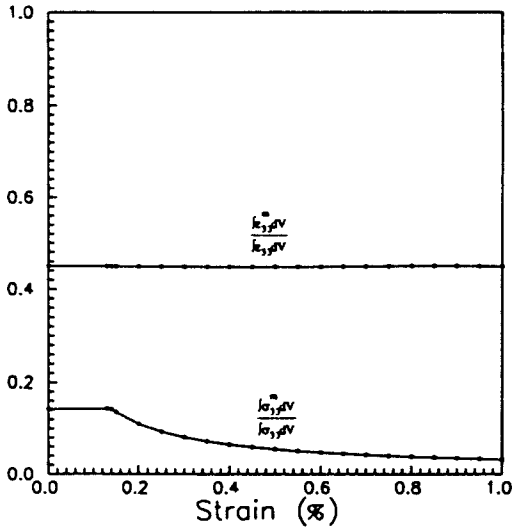

Fig. 9. Normalized contributions of stress and strain from the matrix phase for longitudinal tension.

3.5. *Averages of stress and strain*

The contributions from the matrix phase to the average stress and strain are shown in Fig. 9 for longitudinal tension. The sums of the ratios for fiber and matrix are equal to one. The calculations show that the strain ratio remains constant during the loading and is equal to the volume fraction. This indicates a nearly constant longitudinal strain component in the composite while the stress ratio decreases after matrix yield. Loadings that do not directly stress the fibers in the longitudinal direction exhibit the same features as those shown in Fig. 10 for inplane shear. The ratio between average stress in matrix and fiber remains approximately constant during the deformation while the matrix strain ratio increases after matrix yield. The ratio of the average stress in the matrix is lower than the matrix volume fraction. It is equal to the matrix volume fraction when a constant stress field is assumed. This assumption is frequently used in lower bound calculations. In some models it is assumed that the strain is constant in the fiber direction and the ratios between phase averages of the stresses in the other directions remain constant during the deformation. The ratios are given by the linear elastic solution and the constitutive equation for each phase is used to relate the phase averages of stress and strain. Predicted stress–strain curves for the two assumptions are shown in Fig. 11 for inplane shear. Use of the constant

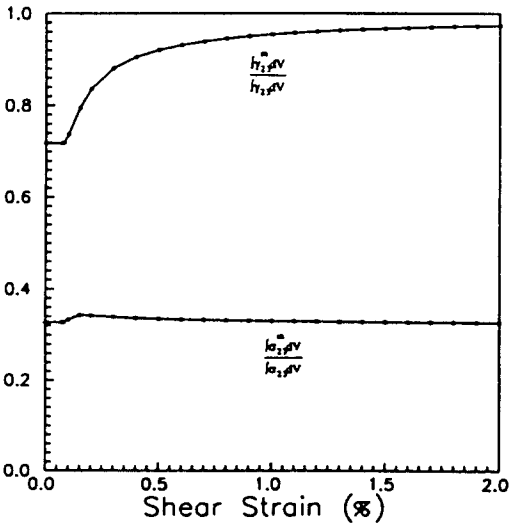

Fig. 10. Normalized contributions of stress and strain from the matrix phase for inplane shear.

ratio between stress phase averages substantially underestimate the plastic deformation in the matrix. The nonlinearity in the constitutive equation causes the actual non-uniform stress distribution in the matrix to give a much higher strain contribution than the average stress. The assumption of a constant stress overestimates the matrix stress and overpredicts the strain.

3.6. *Plastic zones*

The evolution of the plastic zone in the matrix is dependent on the loading direction and is shown for transverse tension in the 1-direction in Fig. 12 and for tension in the 2-direction in Fig. 13. For σ_{11} loading, yielding starts at the fiber matrix interface at an angle of 60° from the tensile loading direction. Increased loading develops a contained region of yielded matrix that extends in the loading direction between the fibers. Further loading causes a growth of the plastic zone such that it extends from one side of the unit cell to the other side perpendicular to the tensile direction and this coincides with noticeable plastic deformation of the composite. Some symmetry locations do not yield for a limited global strain. For σ_{22} loading, Fig. 13, initial yielding occurs simultaneously at two locations: at the interface at an angle of 30° to the tensile direction and in the middle of the matrix between the poles of the fibers. It can be concluded that the initial details of the development of the plastic zone are dependent on the loading direction but the subsequent trend is similar.

3.7. *Initial yield surface*

The initial yield surface for the composite has been determined by superimposing the linear elastic stress distributions for the different load cases and calculating the von Mises equivalent stress.

Calculated initial yield surfaces for inplane shear are shown in Fig. 14 for different orientations of the unit cell. Initial yield always occurs at the interface for this loading. For the stresses σ_{11} and σ_{III} orientated in the principal directions of the material, $\nu = 0$ in Fig. 2b, the yield surface has the shape of a hexagon. This shape was also found by Dvorak *et al.* (1974). The real composite is transversely isotropic and its yield surface has the form of a circle in this plane (this can be determined from the form of the invariants in Appendix B). One way to use the results from the hexagonal array is to assume that the unit call can be oriented in any direction in relation to the global stress state. The initial yield surface is then dictated by the unit cell orientated with the highest stress concentration so that the yield surface is minimized giving the inscribed circle in Fig. 14. This approach requires that the stress concentrations must be evaluated for many load combinations to determine the

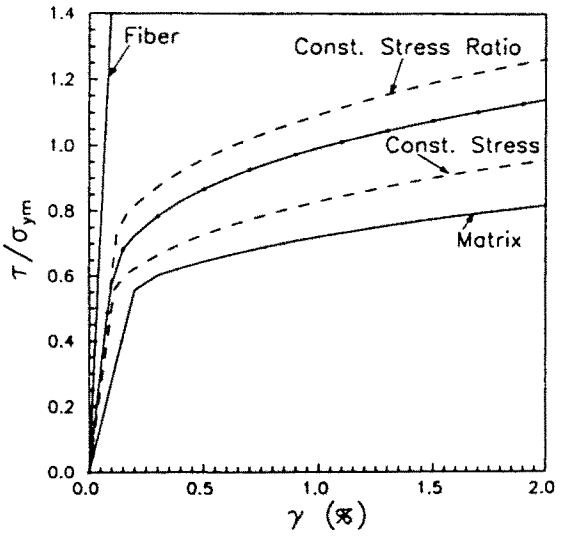

Fig. 11. Estimated inplane shear stress–strain curves for the assumptions: constant stress field, the ratio between the phase averages of stress is given by the linear elastic stress distribution.

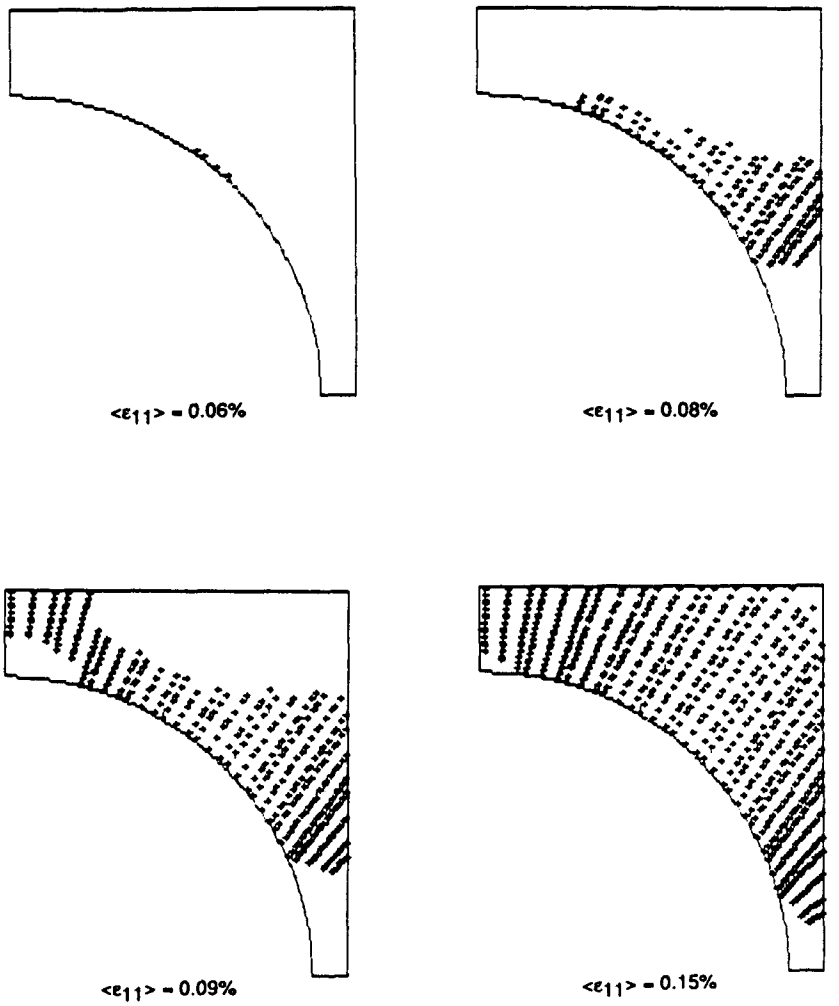

Fig. 12. Development of plastic zone in matrix for transverse tension in the 1-direction.

yield surface for the general stress state. A less time consuming and more pleasing method is to assume that the principal stresses in the transverse plane and σ_{I3} and σ_{II3} are orientated at an angle of 15° to the symmetry lines of the hexagonal array, corresponding to the I and II in Fig. 2b with $\upsilon = 15°$. The advantage is that the two orthogonal loading directions I and II are identical with the same micro-structure and the hexagonal cell has the desired symmetry properties of a transversely isotropic material for this loading.

Initial yield surfaces for transverse loading are shown in Fig. 15. The surface for loadings in the 1 and 2 directions, $\upsilon = 0$, do not have the symmetry properties of a transversely isotropic material. The yield surface is smaller in the σ_{22} direction than in the σ_{11} direction. The location of maximum equivalent stress in the matrix was found to be either at the interface or in the middle between two fibers depending on the loading. The shape of the yield surface corresponding to a unit cell orientated in the direction giving the highest stress concentration and the one corresponding to the principal stresses in the 15° directions are also shown. They do not differ greatly in shape but the latter is far easier to determine. The maximum effective stress was always located on the interface for the surface $\upsilon = 15°$. The shape of the initial yield surface, $\upsilon = 15°$, in σ_{II}, σ_{III} and σ_{33} space is given in Fig. 16. The surface is thin in the direction $\sigma_{II} = -\sigma_{III}$, corresponding to transverse shear, and is long in the direction $\sigma_{II} = \sigma_{III}$ with a sharp corner. Longitudinal and transverse biaxial loading with stress components of equal sign load the fiber in the longitudinal direction and this causes a high yield stress. Transverse tension and transverse and inplane shear do not load the fiber strongly in the longitudinal direction and the initial yield stress

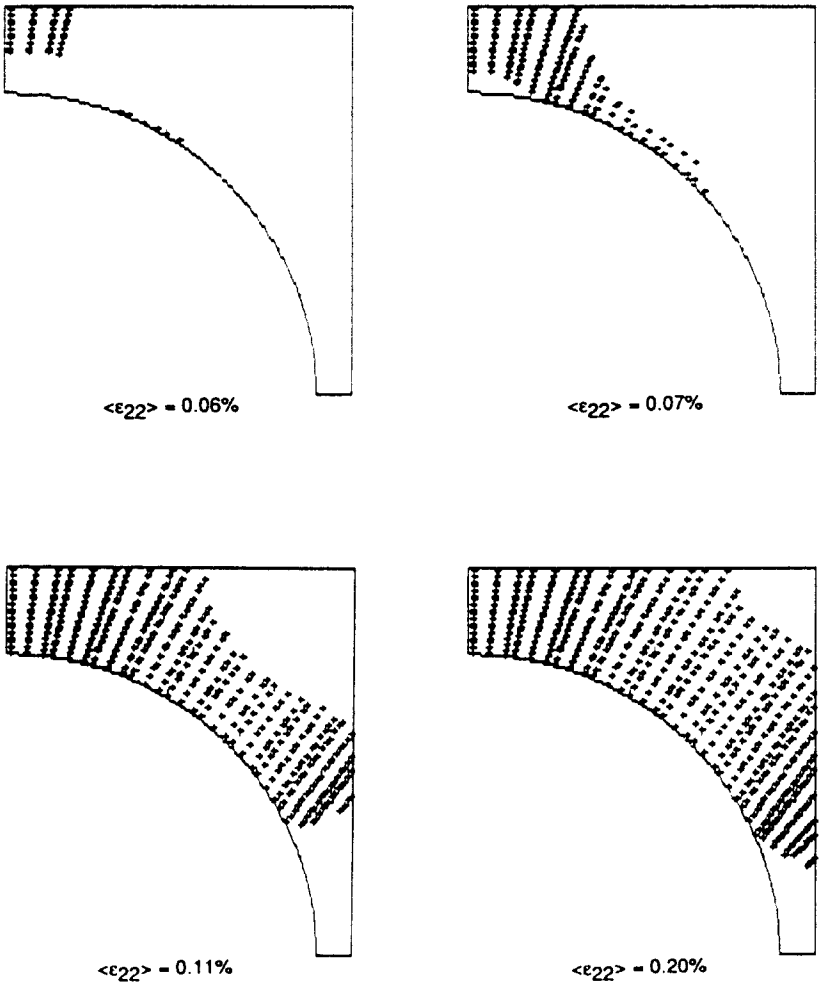

Fig. 13. Development of plastic zone in matrix for transverse tension in the 2-direction.

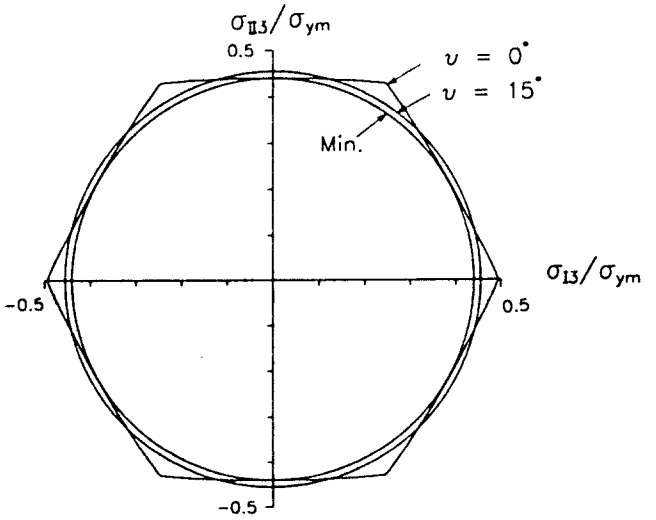

Fig. 14. Initial yield surface for inplane shear loading.

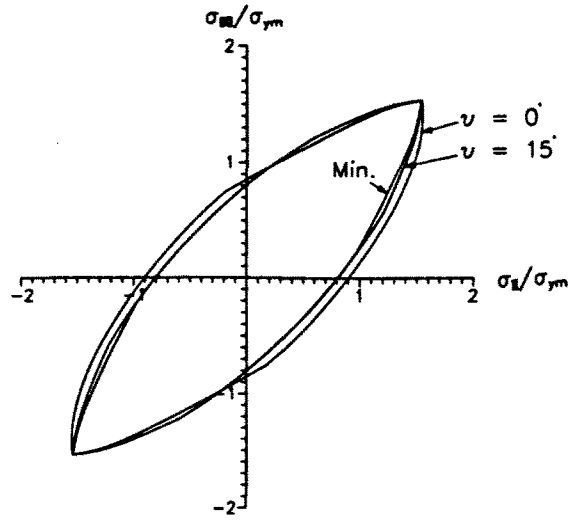

Fig. 15. Initial yield surface for transverse loading.

is lower than for the matrix due to the stress concentrations induced by the fiber. The plastic zones at the initial plastic deformation are contained, Figs 12 and 13, and the initial yielding causes very small average plastic strains for the composite.

4. CONCLUSIONS

The effective properties for a composite with a periodic micro-structure consisting of nonlinear constituents is governed by a unit cell problem when the length scale of the micro-structure is short in comparison to the wavelength of the loading.

The nonlinear transverse and inplane shear strain responses for fiber reinforced composites are strongly affected by the arrangement of the fibers in the transverse plane while the linear elastic constants are less dependent on the arrangements. This implies that care must be exercised when periodic arrays are used to model the behavior composites with randomly distributed reinforcements. This is especially true when the matrix has a high hardening exponent.

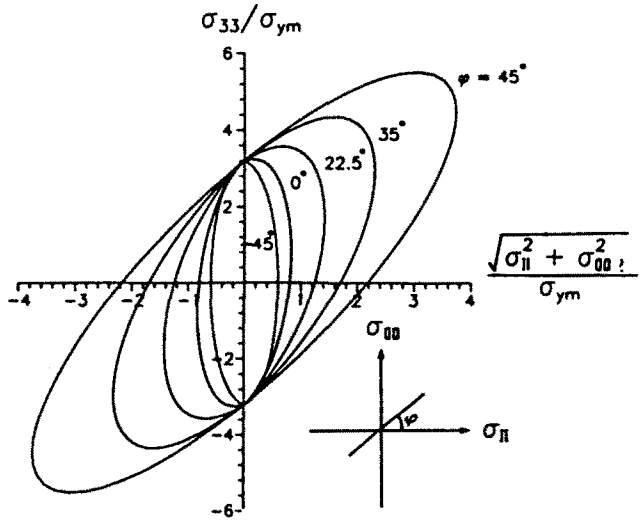

Fig. 16. Initial yield surface for combined transverse and longitudinal loading. It is calculated by assuming that the principal stresses in the transverse plane are orientated at an angle of 15° to the symmetry planes.

The hexagonal array is frequently used to model the behavior of transversely isotropic materials because its linear elastic response is transversely isotropic. It was demonstrated that the responses of the array to loadings that are not axisymmetric with respect to the fibers is not transversely isotropic. This was most noticeable for inplane shear. In order to get reasonable results loading directions must be evaluated which avoid slip unconstrained by the fibers.

The initial yield surface of the hexagonal array is not transversely isotropic. A transversely isotropic yield surface can be determined efficiently from the hexagonal array by assuming that the principal stresses are orientated 15° to the principal directions of the material, Fig. 2b. This concept can also be used in models when hexagonal grains are used to model creep by grain boundary sliding and diffusion in order to get an isotropic behavior.

The calculations showed that the longitudinal strain is approximately constant in the composite and that the phase averages of transverse stresses and inplane shear stresses remain constant during the loading.

Acknowledgement—This work has been supported in part by Chrysler Challenge Funds from Chrysler Corporation and by a grant from NASA Lewis Research Center.

REFERENCES

Adams, F. D. (1970). Inelastic analysis of a unidirectional composite subjected to transverse normal loading. *J. Comp. Mater.* **4**, 310–328.

Adams, F. D. and Tsai, S. W. (1969). The influence of random filament packing on the transverse stiffness on unidirectional composites. *J. Comp. Mater.* **3**, 368–381.

Burns, S. (1989). Private communications. Department of Theoretical and Applied Mechanics, University of Illinois at Urbana Champaign.

Chen, C. H. and Cheng, S. (1967). Mechanical properties of fiber reinforced composites. *J. Comp. Mater.* **1**, 30–41.

Christensen, R. M. (1979). *Mechanics of Composite Materials*. Wiley, New York.

Christensen, R. M. (1987). Lawrence Livermore Laboratory, report mms 14.

Dvorak, G. J., Rao, M. S. M. and Tarn, J. Q. (1974). Yielding in unidirectional composites under external loads and temperature changes. *J. Comp. Mater.* **7**, 194–205.

Green, A. H. and Adkins, J. E. (1960). *Large Elastic Deformations*. Clarendon Press, Oxford.

Hashin, Z. (1983). Analysis of composite materials—a survey. *ASME J. Appl. Mech.* **50**, 481–505.

Hutchinson, J. W. and Neal, K. W. (1981). Finite strain J_2 deformation theory. In *IUTAM Symposium on Finite Elasticity* (Edited by D. E. Carlson and R. T. Shield). Martinus Nijhoff, The Hague.

Jansson, S. (1986). Fully plastic plane stress solutions for biaxially loaded center-cracked plates. *ASME J. Appl. Mech.* **53**, 555–560.

Jansson, S. (1991). Mechanical characterization and numerical modeling of non-linear deformation and fracture of a fiber reinforced metal matrix composite. *Mech. Mater.* **12**, 47–62.

Jones, R. M. (1974). *Mechanics of Composite Materials*. Scripta Book Company, Washington, DC.

Keller, J. B. (1976). Effective behavior of heterogeneous media. In *Statistical Mechanics and Statistical Methods in Theory and Application* (Edited by U. Landman). Plenum Press, New York.

Larson, E. W. (1976). Neutron transport and diffusion in inhomogeneous media. II. *Nucl. Sci. Engng* **60**, 357–368.

Len'e, F. (1986). Damage constitutive relations for composite materials. *Engng Fract. Mech.* **25**, 713–728.

Len'e, F. and Leguillon, D. (1982). Homogenized constitutive law for a partially cohesive composite material. *Int. J. Solids Structures* **18**, 443–458.

Suquet, P. M. (1983). Local and global aspects in the mathematical theory of plasticity. In *Plasticity Today: Modeling, Methods and Applications* (Edited by A. Sawczuk and G. Bianchi). Elsevier, London.

Suquet, P. M. (1985). Approach by homogenization of some linear and nonlinear problems in solid mechanics. In *Plastic Behavior of Anisotropic Solids* (Edited by J. Bohler). Center National De La Recherche Scientifique, Paris.

APPENDIX A

The considered loadings coincide with the principal directions of the material. The periodic displacement field is taken to be zero at the center of the unit cell for the square array. This implies that the symmetric unit cell is subjected to symmetric or antisymmetric loading and only a quarter of the unit cell has to be analysed.

Longitudinal loading, $\langle \sigma_{11} \rangle \neq 0$, is imposed by specifying the strain ε^0_{11}. The resulting displacement is symmetric with respect to the y_1 and y_2 axes and the normal components of the field have to be zero along these axes, giving

$$u_1(y_1 = 0) = u_2(y_2 = 0) = 0.$$

The symmetry of the loading together with the periodicity of the displacement field require $u_1(y_1 = b) = 0$ and $u_2(y_2 = b) = 0$. However, the conditions of $\langle \sigma_{11} \rangle = 0$ and $\langle \sigma_{22} \rangle = 0$ are automatically satisfied by the solution procedure by letting these boundaries displace with constant normal displacement such that

$$u_1(y_1 = b) = \text{constant} \quad \text{so} \quad \int_{y_1=a} T_1 \, d\Gamma = 0$$

$$u_2(y_2 = b) = \text{constant} \quad \text{so} \quad \int_{y_2=a} T_2 \, d\Gamma = 0$$

where T_i is the traction on the boundary Γ of the unit cell. The average strains ε^0_{11} and ε^0_{22} are then such that $\langle\sigma_{11}\rangle = \langle\sigma_{22}\rangle = 0$, *cf.* eqn (25).

Transverse loading, $\langle\sigma_{11}\rangle \neq 0$, is imposed by specifying ε^0_{11}. The symmetry of the loading together with the periodicity of the displacement field require

$$u_1(y_1 = 0) = u_{,2}(y_2 = 0) = u_1(y_1 = b) = 0.$$

The condition of $\langle\sigma_{22}\rangle = 0$ is accomplished by letting the normal displacement of the boundary $y_2 = a$ be constant such that

$$u_2(y_2 = b) = \text{constant} \quad \text{so} \quad \int_{y_2=a} T_2 \, d\Gamma = 0$$

and the longitudinal strain is given by the condition

$$\varepsilon^0_{33} = \text{constant} \quad \text{so} \quad \int_{y_1=0} T_3 \, d\Gamma = 0.$$

Transverse shear, $\langle\sigma_{12}\rangle \neq 0$, is antisymmetric with respect to the y_1 and y_2 axes, requiring

$$u_1(y_2 = 0) = u_2(y_1 = 0) = 0.$$

The antisymmetry of the loading together with the periodicity of the displacement field require

$$u_1(y_2 = b) = u_2(y_1 = b) = 0.$$

For inplane shear, $\langle\sigma_{13}\rangle \neq 0$, is the out of plane displacement u_3 the only non-vanishing component. The loading is symmetric with respect to the y_1 axis and antisymmetric with respect to the y_2 axis and this together with the periodicity of the displacement field requires

$$u_3(y_1 = 0) = u_3(y_2 = b) = 0.$$

The hexagonal unit cell can also be reduced to a quarter of its initial size by using the same symmetry arguments as for the square array. The upper right quarter, Fig. 2b, has an additional inversion symmetry around the point $(y_1 = \sqrt{3}/2\, b,\ y_2 = 1/2\, b)$ when the periodic displacement field is fixed at this point and this makes it possible to reduce the problem to an eighth of its original size. The inversion symmetry along the line $y_1 = \sqrt{3}/2\, b$ is given by the following conditions:

$$u_i(y_1 = \sqrt{3}/2\, b,\ y_2 = 1/2\, b + e) = -u_i(y_1 = \sqrt{3}/2\, b,\ y_2 = 1/2\, b - e)$$
$$T_i(y_1 = \sqrt{3}/2\, b,\ y_2 = 1/2\, b + e) = T_i(y_1 = \sqrt{3}/2\, b,\ y_2 = 1/2\, b - e)$$

where

$$0 \leqslant e \leqslant b/4.$$

The derivations of the remaining boundary conditions are similar to the derivations for the square array and in addition to the inversion symmetry are the following boundary conditions imposed for the different loadings:

$\langle\sigma_{33}\rangle \neq 0$:

$$u_1(y_1 = 0) = \text{constant} \quad \text{so} \quad \int_{y_1=0} T_1 \, d\Gamma = 0$$

$$u_2(y_2 = 0) = -u_2(y_2 = b) \quad \text{so} \quad \int_{y_2=0} T_2 \, d\Gamma - \int_{y_2=b} T_2 \, d\Gamma = 0.$$

$\langle\sigma_{11}\rangle \neq 0$:

$$u_1(y_1 = 0) = 0, \qquad u_2(y_2 = 0) = -u_2(y_2 = \sqrt{3}/2\, b) = \text{constant} \quad \text{so} \quad \int_{y_2=0} T_2 \, d\Gamma - \int_{y_2=b} T_2 \, d\Gamma = 0$$

$$\varepsilon_{33} = \text{constant} \quad \text{so} \quad \int_{y_1=0} T_3 \, d\Gamma = 0.$$

$\langle\sigma_{22}\rangle \neq 0$:

$$u_1(y_1 = 0) = \text{constant} \quad \text{so} \quad \int_{y_1=0} T_1 \, d\Gamma = 0, \qquad u_2(y_2 = 0) = u_2(y_2 = h) = 0,$$

$$\varepsilon_{11} = \text{constant} \quad \text{so} \quad \int_{y_1=0} T_2 \, d\Gamma = 0.$$

$\langle\sigma_{12}\rangle \neq 0$:

$$u_2(y_1 = 0) = u_1(y_2 = 0) = u_1(y_2 = h) = 0.$$

$\langle\sigma_{13}\rangle \neq 0$:

$$u_3(y_1 = 0) = 0.$$

$\langle\sigma_{23}\rangle \neq 0$:

$$u_3(y_2 = 0) = u_3(y_2 = h) = 0.$$

APPENDIX B

The following stress invariants [*cf.* Green and Adkins (1960)] are derived from a polynomial basis and the symmetry relation $\sigma_{ij} = \sigma_{ji}$ of the stress tensor have been used. The invariants are not unique but irreducible.

Square array:

$$\sigma_{11}+\sigma_{22}, \quad \sigma_{33}, \quad \sigma_{12}^2, \quad \sigma_{11}\sigma_{22}, \quad \sigma_{13}^2+\sigma_{23}^2, \quad \sigma_{12}\sigma_{13}\sigma_{23}, \quad \sigma_{11}\sigma_{23}^2+\sigma_{22}\sigma_{13}^2, \quad \sigma_{13}^2\sigma_{23}^2.$$

Hexagonal array:

$$\sigma_{11}+\sigma_{22}, \quad \sigma_{33}, \quad (\sigma_{11}-\sigma_{22})^2+4\sigma_{12}^2, \quad \sigma_{13}^2+\sigma_{23}^2,$$

$$\sigma_{11}(\sigma_{11}^2+9\sigma_{22}^2-12\sigma_{12}^2+6\sigma_{11}\sigma_{22}), \quad \sigma_{11}\sigma_{23}^2+\sigma_{22}\sigma_{13}^2-2\sigma_{12}\sigma_{13}\sigma_{23},$$

$$(\sigma_{11}^2-3\sigma_{22}^2+4\sigma_{12}^2+2\sigma_{11}\sigma_{22})\sigma_{13}^2-2(\sigma_{11}^2+3\sigma_{11}\sigma_{22})(\sigma_{13}^2+\sigma_{23}^2)-8\sigma_{11}\sigma_{12}\sigma_{13}\sigma_{23},$$

$$\sigma_{11}\sigma_{13}^4+3\sigma_{11}\sigma_{23}^4+2\sigma_{22}\sigma_{13}^4+6\sigma_{22}\sigma_{13}^2\sigma_{23}^2-8\sigma_{12}\sigma_{13}^3\sigma_{23}, \quad \sigma_{11}(\sigma_{13}^2-3\sigma_{23}^2)^2.$$

Transversely isotropic:

$$\sigma_{11}+\sigma_{22}, \quad \sigma_{33}, \quad (\sigma_{11}-\sigma_{22})^2+4\sigma_{12}^2, \quad \sigma_{13}^2+\sigma_{23}^2, \quad |\sigma_{ij}|.$$